Oxidation of dissolved organic matter in the effluent of a sewage treatment plant using ozone combined with hydrogen peroxide (O_3/H_2O_2)

Roberto Rosal, Antonio Rodríguez, José Antonio Perdigón-Melón, Alice Petre, Eloy García-Calvo, Oxidation of dissolved organic matter in the effluent of a sewage treatment plant using ozone combined with hydrogen peroxide (O3/H2O2), Chemical Engineering Journal, Volume 149, Issues 1–3, 1 July 2009, Pages 311-318

https://doi.org/10.1016/j.cej.2008.11.019

Oxidation of dissolved organic matter in the effluent of a sewage treatment plant using ozone combined with hydrogen peroxide (O_3/H_2O_2)

Roberto Rosal*, Antonio Rodríguez, José Antonio Perdigón-Melón, Alice Petre and Eloy García-Calvo

Department of Chemical Engineering, Universidad de Alcalá, 28771 Alcalá de Henares, Spain.

* Corresponding author: roberto.rosal@uah.es

Abstract

The effluent from the secondary clarifier of an Urban Sewage Treatment Plant was oxidized by the combined and simultaneous use of ozone and hydrogen peroxide. The purpose was to increase the wastewater's reuse potential by improving water quality. The removal of dissolved organic chemicals was enhanced by adding periodic pulses of hydrogen peroxide while keeping pH above 8.0 throughout the runs. These conditions led to almost complete mineralization in less than one hour. Under similar conditions, without the addition of hydrogen peroxide, the removal of total organic carbon (TOC) was no higher than 35%. The evolution of TOC was related to the concentration of hydroxyl radicals using a second-order kinetic model in which the exposure to hydroxyl radical was included by assuming a quasi-steady-state approximation. The concentration of hydroxyl radical was computed using the experimental data from ozone and hydrogen peroxide. The kinetic constants for the hydroxyl-mediated mineralization process were determined for wastewaters collected during a one-year sampling campaign. The results showed that the mineralization process takes place in two periods whose rate constants were linked to the chemical oxygen demand (COD) to biochemical oxygen demand (BOD) ratio and to the chloride content of wastewaters. During the first part of the runs, the specific rate of mineralization was high, before subsequently decreasing after a period of 5-15 min by an average factor of 6.4 whose 95% confidence interval was in the 3.4-9.3 range. The moles of TOC removed per mole of ozone consumed were in the range of 9.2-17.7 mg O_3/mg TOC measured at maximum ozone efficiency, which always occurred within the first ten minutes.

Keywords: Ozonation, Hydrogen Peroxide, Advanced Oxidation Processes, Water Pollution Control, Water Reuse, Kinetics.

1. Introduction

The environmental protection of surface and groundwater, including artificial and heavily modified bodies of water, has been urged upon Member States of the European Union by the EC Water Framework Directive [1]. The aim is to achieve good ecological water status in terms of the presence of chemicals from human activity in a period covering the fifteen years from the date this Directive comes into force (2015). In this connection, increasing water scarcity enhances wastewater reuse, especially that geared towards the large amount of effluents from Sewage Treatment Plants (STP) currently discharged to surface bodies. Possible reuse targets for biotreated municipal wastewater include industrial, agricultural and domestic uses. Any of these reuse options require different water qualities, but in general tertiary treatments must be implemented after the secondary settling of activated sludge treatments to avoid the presence of organic pollutants in treated waters [2]. Certain regulations include TOC as a quality parameter for practices of indirect potable reuse such as spreading basins or injection [2]. Organic compounds, even in very low amounts, severely endanger water reuse in many applications. This is the case of endocrine-disrupting compounds and other emerging pollutants that are only partially removed from wastewater in conventional wastewater treatments in the STPs and whose presence is repeatedly reported in effluents [4-8].

For the removal of organic compounds in wastewater, ozone-based Advanced Oxidation Processes (AOP) are much more efficient than ozone alone. The addition of H_2O_2 or UV radiation accelerates the decomposition of ozone due to the increased rate of hydroxyl radical generation [9]. Less severe oxidation processes, like ozonation in acidic conditions, have been reported to yield reaction intermediates that could exhibit enhanced toxicity to microorganisms in early stages of oxidation [10-11]. This problem can be overcome by AOP, which are deliberately aimed at the complete oxidation of recalcitrant compounds, thus yielding less harmful or easily biodegradable products [12]. Certain combinations of AOPs have been proposed with a view to increasing the capacity to treat refractory pollutants or to achieve a deeper degree of mineralization [13]. Among others, Fenton, photo-Fenton, photocatalysis on TiO_2, ultraviolet-based oxidation processes (H_2O_2/UV and O_3/UV), and the ozone based O_3/HO^- and O_3/H_2O_2 have been reported by different authors [14-16]. All of these involve the generation of hydroxyl radicals, a highly reactive and unselective species, in sufficient amounts to

oxidize the organics in wastewater. O_3/H_2O_2 belongs to the group of chemical AOP and produces HO· radicals through a sequence of reactions initiated by hydroperoxide anion, the conjugate base of hydrogen peroxide [17-19]. The use of the O_3/H_2O_2 system was shown to ensure a high degree of mineralization [20]. This feature was sought in order to ensure the absence of any oxidation intermediates and a reduction in toxicity, as well as the removal of persistent, emerging or any other individual pollutant from the many compounds identified in STP effluents [21].

This work focuses on the need to provide adequate quality in order to broaden water reuse practices. It is a part of a program financed by the Spanish Government that is undertaking a complete study of the different aspects involved in the reuse of wastewater consistent with the fact that reclamation and reuse practices require careful planning steps. These include the application of advanced oxidation technologies for the use of reclaimed water and the assessment of the fate of chemicals during treatments. This work presents results concerning a one-year sampling campaign undertaken in the urban STP of Alcalá de Henares (Madrid, Spain), whose wastewaters were treated using an ozone-based AOP to remove organic compounds. The aim was to establish operational boundaries for AOP in wastewater by relating the extent of mineralization to matrix effects associated with seasonal variability, as well as to contribute to the understanding and modelling of O_3/H_2O_2 technology as applied to wastewater reuse. The rate and extent of mineralization in conditions of alkaline O_3/H_2O_2 advanced oxidation was studied by accurately monitoring dissolved ozone as the key measured variable in the system. An analysis of the ozone effectiveness was derived from the model in order to furnish a basis for the implementation of dosing and control strategies as well as further life cycle analysis [21].

Experimental section

Materials and ozonation procedure

Wastewater was collected from the secondary clarifier of a STP located in Alcalá de Henares (Madrid) that receives a mixture of domestic and industrial wastewater from facilities located around the city. This STP has a capacity of 375000 equivalent inhabitants and is designed to treat a maximum volume of wastewater of 3000 m^3/h. Besides conventional activated sludge treatment, it has recently implemented a biological nutrient removal process to enhance the elimination of phosphorous and nitrogen. All samples were composites of 1-L aliquots collected on an hourly basis during 24 h sampling periods distributed over one year from February to December. Samples were immediately processed or stored in a refrigerator (< 4ºC) inside glass bottles. The ozonation runs were performed in batch mode in a 5-L glass jacketed reactor at 25ºC. The temperature was controlled by a Huber Polystat cc2 and monitored throughout the experiment by means of a Pt100 Resistance Thermometer Detector (RTD). Ozone was produced by a corona discharge ozonator (Ozomatic, SWO100) fed by an AirSep AS-12 PSA oxygen generation unit. The gas containing ozone was bubbled into the liquid by means of a porous glass disk with a gas flow of 0.36 Nm^3/h. The concentration of ozone in the gas was ~ 45 g Nm^{-3} and measured immediately before each run. The off-gas was vented to an ozone destruction unit. The reaction vessel was agitated with a Teflon four-blade impeller at 1000 rpm. During the runs, injections of 0.15 mL of H_2O_2 (30 % w/v Sigma-Aldrich) were performed every 5 min starting at the beginning of ozone bubbling. This amount was chosen in order to keep the overall H_2O_2/O_3 molar ratio lower than 0.5 in agreement with other published data and the overall stoichiometry of the O_3-H_2O_2 reaction [22-23]. Pulses were intended to avoid a great excess of hydrogen peroxide, well-known radical scavenger of hydroxyl radicals [25]. Some runs were performed in the absence of hydrogen peroxide in conditions of alkaline ozonation with pH > 8.5 and without any injection of hydrogen peroxide. Additional details on the experimental set-up are given elsewhere [26, 27]

During the runs, certain samples were withdrawn for analysis after previously removing ozone by bubbling nitrogen in order to prevent further oxidation reactions. The experiments started at pH 8.5 and were always kept above 8.0 by pumping a diluted solution of sodium hydroxide (Panreac) with a feed-back PID control device when necessary. The decomposition of ozone acidified the reaction mixture but the general trend during most of the run was a moderate increase of pH. This effect was attributed to reactions between hydroxyl radicals and carbonate and bicarbonate ions formed during the mineralization process [28].

Analysis

The concentration of dissolved ozone was measured by means of an amperometric Rosemount 499A OZ analyser calibrated against the Indigo Colorimetric Method (SM 4500-O_3 B). The signal, transmitted by a Rosemount 1055 SoluComp II Dual Input Analyser was recorded by means of a data acquisition unit. The concentration of ozone in gas phase was measured using an Anseros Ozomat GM6000 Pro photometer calibrated against a chemical method [29]. The pH of the reaction mixture was measured by means of a CRISON electrode connected to a Eutech αlpha-pH100 feed-back control system whose final control element was a LC10AS Shimadzu pump delivering a solution of sodium hydroxide. The signals from the concentration of dissolved ozone, pH and temperature were recorded by means of an Agilent 34970 Data Acquisition Unit connected to a computer with a sampling period of 5 s.

Total Organic Carbon (TOC) analyses were performed with the aid of a Shimadzu TOC-VCSH analyzer equipped with ASI-V autosampler. Inorganic anions were determined using a Dionex DX120 Ion Chromatograph with conductivity detector and an IonPac AS9-HC 4x250mm analytical column with ASRS-Ultra

suppressor. The eluent was 9.0 mM Na_2CO_3 with a flow of 1.0 mL/min. Inorganic cations were determined by an IonPac CS512A 4 x 250 mm cation exchange analytical column with Dionex CSRS Ultra II suppressor and 20 mM metasulphonic acid as eluent. Total suspended solids were determined by the American Public Health Association (APHA) Method 2540 D, "Total Suspended Solids Dried at 103–105°C". The determination of COD followed APHA Method 5220 C. For BOD-5 analysis APHA 5210 B was used with a commercially available nitrification inhibitor (Hach, 2533). Standard Methods SM 4500-P E and 4500 NH_3 D were used for the determination of ortho-phosphate and ammonia. Hydrogen peroxide was determined by Eisenberg's colorimetric method, which uses titanium sulphate to create with hydrogen peroxide a yellow peroxo-complex measured at 405 nm [30].

Results and discussion

Characterization of wastewater

Table 1 shows the main parameters of wastewater samples with separate averages and standard deviations for wet and dry periods. The same parameters in ozonated samples are also indicated. Fig. 1, representing the profiles of COD and BOD, shows parallel behaviour in the wet season, with considerably higher COD contents during summer, corresponding to samples taken between days 120 and 240. TOC in Table 1 was determined in settled and filtered samples and therefore corresponds entirely to dissolved organic carbon. The results of TOC with non-filtered samples led to an average value of COD/TOC of 4.8 ± 2.6 (95% boundary), indicating a relatively low biodegradability whose origin could be attributed to the load of industrial wastewater received by the STP. The evolution of chloride is shown in Fig. 5b. During the sampling period, which lasted almost the whole of 2007, the plant worked in conditions of reasonable nitrification, with an ammonia nitrogen content in general below 5 mg/L, a content which the ozonation treatment managed to reduce to less than or slightly above 1 mg/L.

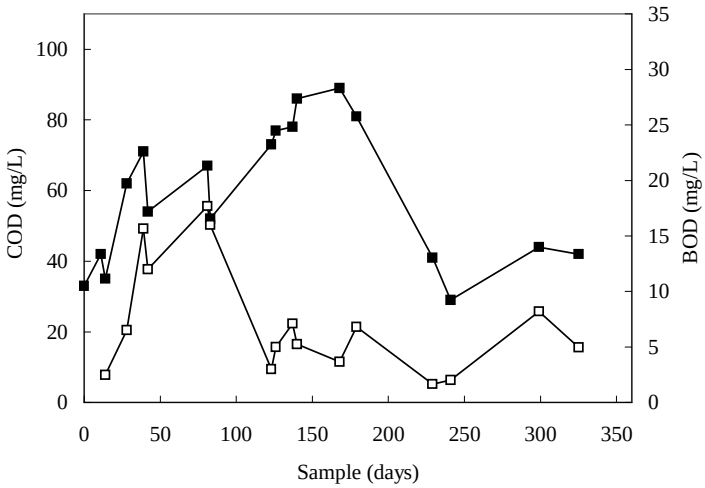

Figure 1. Evolution of COD (■) and BOD (□) during the sampling period. The days from 120 to 240 corresponded to the dry summer period.

Mineralization model

The experiments were conducted in semicontinuous mode with periodic pulses of H_2O_2. Consequently, the molar ratio H_2O_2/O_3 changed during the run. The overall H_2O_2/O_3 ratio was calculated from the maximum rate of ozone transfer from the gas phase:

$$\frac{N\, C_{H_2O_2,o}}{k_L a\, C^*_{O_3}} \qquad (1)$$

where N is the number of pulses, k_La the volumetric mass transfer coefficient, $C_{H_2O_2,o}$ the initial concentration of

Table 1. Seasonal variation of wastewater parameters and data from ozonated samples.

Parameters	Spring-Winter (November-June)	Summer-Autumn (July-October)	Treated samples
pH	7.65 (0.24)	7.56 (0.17)	-
Total Suspended Solids (mg/L)	8.6 (5.7)	3.0 (1.3)	7.8 (5.2)
Turbidity (NTU)	7.4 (5.5)	3.3 (0.4)	3.7 (0.8)
Conductivity (μS/cm)	573 (140)	640 (74)	600 (130)
COD (mg/L)	59 (19)	60 (26)	28 (23)
BOD_5 (mg/L)	12.7 (10.9)	7.3 (5.7)	1.9 (1.1)
TOC (mg/L)	8.6 (2.8)	6.6 (2.4)	0.9 (0.7)
PO_4-P (mg/L)	1.92 (1.4)	0.78 (0.12)	2.00 (1.52)
NO_3-N (mg/L)	3.50 (3.14)	7.4 (0.67)	n.d.
Sulfate (mg/L)	111 (42)	99 (25)	102 (32)
Chloride (mg/L)	72.8 (11.1)	99.2 (3.9)	81 (12)
Sodium (mg/L)	59.2 (9.4)	72.8 (6.5)	62 (8.8)
Potassium (mg/L)	11.2 (1.3)	13.3 (2.5)	10.8 (1.5)
Magnesium (mg/L)	16.9 (8.1)	17.4 (6.2)	16.8 (7.3)
Calcium (mg/L)	36.7 (9.8)	46.5 (7.5)	39.4 (8.1)
Alkalinity (mg/L $CaCO_3$)	434 (62)	361 (31)	n.d.

Standard deviations in parenthesis, n.d.: not determined.

equilibrium concentration of ozone in the liquid calculated from Henry's law [31]. The mass transfer coefficient was determined in transient runs with pure water and yielded a value of $k_La = 0.010 \pm 0.005$ s^{-1}. For the experimental conditions used in this work, the ratio of Eq. (1) was in the 0.35-0.45 range, near the optimum found by Paillard et al. [32]. This ratio was kept below stoichiometry in order to account for the higher reactivity of ozone with organic matter and inorganics with respect to hydrogen peroxide, as well as to limit the extent of radical scavenging due to the reaction between hydroxyl radical and hydrogen peroxide [33].

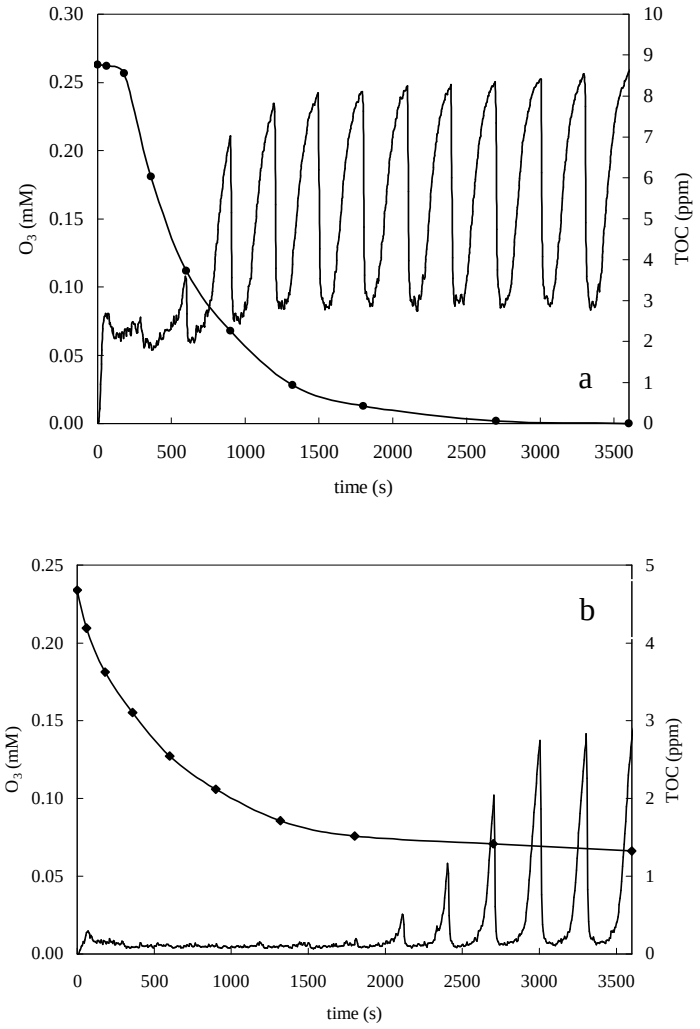

Figure. 2. Evolution of TOC (●) and concentration of dissolved ozone during the treatment of wastewater with repeated injections of 0.15 mL of H_2O_2 (30 % w/v) every 300 s. Samples taken (a) in April, (b) in September.

The behaviour of wastewater samples during ozonation revealed strong seasonal differences. Fig. 2 shows TOC and ozone profiles for two representative runs treated in spring (April, Fig. 2a) and during the dry summer period (September, Fig 2b). In most cases, the concentration of dissolved ozone rapidly declined after the injection of hydrogen peroxide, a usual pattern that was observed only after an extended ozonation period in samples taken during the summer. In all cases, the concentration of dissolved ozone is different from zero suggesting that the kinetic regime is slow. The higher values for Hatta numbers, corresponding to the injection of hydrogen peroxide, can be obtained from the following expression, already simplified by considering that pH << pK_a:

$$Ha = \frac{\sqrt{k_{HO_2^-}\ 10^{pH-pK_a}\ C_{H_2O_2,o}\ D_{O_3}}}{k_L} \qquad (2)$$

where D_{O_3} is the diffusivity of ozone in water (1.77×10^{-9} m^2 s^{-1}), k_i the specific rate of the reaction between ozone and hydrogen peroxide and $pK_a = 11.75$ for H_2O_2. The value of $k_L = 5.5 \times 10^{-5}$ m s^{-1} was evaluated according to Calderbank and Moo-Young [34]. In all cases Ha < 0.10 and the kinetic regime was slow, a finding consistent with the fact that ozone was detected in solution at any time during runs.

The pattern of TOC removal revealed differences among samples, although these were not dependent on their belonging to wet or dry periods. The most apparent was the existence of an induction period in some processed samples. Fig. 2b shows a period of about 3 min during which the dissolved organic carbon was almost unaffected by O_3/H_2O_2. This behaviour appeared in all samples with low COD/BOD ratio, a variable that turned out to be particularly linked to the mineralization kinetics. In the rest of the runs, the first few minutes of ozonation corresponded to a rapid mineralization period with a still limited concentration of carboxylic acids, the well-known final group of oxidation products.

In contrast with runs carried out with an injection of hydrogen peroxide, alkaline ozonation alone yielded much lower mineralization rates. Alkaline ozonation initiates with the reaction of hydroxide anion with ozone, a reaction whose second order constant is relatively small (70 M^{-1} s^{-1}) compared to that with hydroperoxide anion reported below. Fig. 3 shows the results obtained during the ozonation (pH > 8.5) of two wastewaters together with the concentration profile of dissolved ozone recorded during the run. TOC removal was lower than 35% after one hour whereas hydrogen peroxide-assisted ozonation led to mineralization above 75% in all cases.

Considering that direct ozonation is negligible and, therefore, the oxidation of a given organic compound, P, takes place only by means of the hydroxyl radical, the mass balance to a volume element yields the following expression:

$$-\frac{d\,C_P}{d\,t} = k_P\ C_P\ C_{HO\bullet} \qquad (3)$$

The concentration of hydroxyl radicals can be calculated from its initiation and termination rates with the assumption of steady-state. The reaction starts with the rapid reaction of ozone and hydroperoxide anion:

$$O_3 + HO_2^- \xrightarrow{k_{HO_2^-}} HO_2^\bullet + O_3^{\bullet -} \qquad k_{HO_2^-} = 2.2\,x10^6\ M^{-1}\,s^{-1} \qquad (4)$$

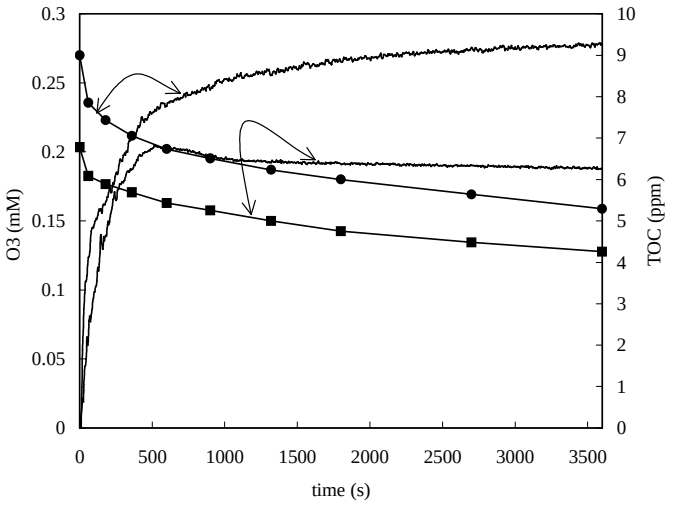

Figure 3. Evolution of TOC and concentration of dissolved ozone during the ozonation treatment of wastewater without injection of hydrogen peroxide for samples taken in April (●) and in June (■).

$$O_3 + HO_2^- \xrightarrow{k_{HO_2^-}} HO_2^\bullet + O_3^{\bullet -} \qquad k_{HO_2^-} = 2.2\,x10^6\ M^{-1}\,s^{-1} \tag{4}$$

Propagation reactions involve the formation of other radical species like $HO_3^\bullet$ that eventually lead to the formation of hydroxyl radicals [19]:

$$O_3^{\bullet -} + H^+ \rightarrow HO_3^\bullet \tag{5}$$

$$HO_3^\bullet \rightarrow HO^\bullet + O_2 \tag{6}$$

$$\frac{d\,C_{HO\bullet}}{d\,t} = 2\,k_{OH^-}\,C_{O_3}\,C_{HO^-} + 2\,k_{HO_2^-}\,C_{O_3}\,C_{HO_2^-} - \sum k_t\,C_S\,C_{HO\bullet} = 0 \tag{7}$$

Immediately after a hydrogen peroxide pulse, a rapid decrease in the concentration of ozone and hydroperoxide anion takes place as a consequence of the rapid reaction between them. Even in such circumstances, the concentration of hydroxyl radical approaches equilibrium very quickly compared with the evolution of other time-dependent variables. The dynamic behaviour of the first-order system described by Eq. 7 depends on the rate constant of termination reactions, the reciprocal of which is the time constant of the system. Considering only termination reactions with carbonate and bicarbonate, whose concentrations in the samples are over 20 and 100 mg $CaCO_3$/L respectively, $\Sigma\,k_t\,C_S \simeq 10^5\ s^{-1}$ and, therefore, the time constant of Eq. 7 is in the order of 10^{-5} s. In other words, the quasi-steady-state hypothesis that consists in assuming that the net rate of hydroxyl formation is zero is borne out by the available kinetic data.

The concentration of HO_2^- can be calculated from pH and pK_a of H_2O_2:

$$C_{HO_2^-} = C_{H_2O_2}\,10^{pH-pK_a} \tag{8}$$

The combination of the preceding equations yields the following expression for the logarithmic decay of the concentration of a given organic pollutant:

$$-\ln\frac{C_P}{C_{P,o}} = k_P\int C_{HO\bullet}\,d\,t = k_P\int\frac{2\,k_{HO_2^-}\,C_{O_3}\,C_{H_2O_2}\,10^{pH-pK_a}}{\sum k_t\,C_S}\,d\,t \tag{9}$$

In this equation, the initiation reaction between ozone and the hydroxide anion, whose specific rate constant is k_{OH^-} = 70 $M^{-1}\,s^{-1}$, was not considered. The high value of $k_{HO_2^-}$ = 2.2 x 10^6 $M^{-1}\,s^{-1}$ makes the contribution of the former about three orders of magnitude lower than the latter and therefore negligible when evaluating the time-integrated concentration of hydroxyl radicals [17-19].

The concentration of hydrogen peroxide can be calculated inside each pulse from the ozone consumed within the liquid phase and that transferred from the gas:

$$C_{H_2O_2} = C_{H_2O_2}(0) - \frac{1}{2}\left[C_{O_3}(0) - C_{O_3}(t)\right] - \frac{k_L a}{2}\left[C^*_{O_3} - C_{O_3}(t)\right]t \tag{10}$$

where $C_{O_3}(0)$ and $C_{O_3}(t)$ are the concentrations of dissolved ozone at the beginning of each pulse of hydrogen peroxide and at any time between pulses. This computation probably overestimates the instantaneous concentration of hydrogen peroxide as it ignores any reaction of hydrogen peroxide other than that with ozone. Instantaneous equilibrium between hydrogen peroxide and hydroperoxide anion was also assumed. The time-integrated concentration of hydroxyl radical must be evaluated after considering the sequence of pulses, where the integral refers to a given pulse in the sequence indicated by the summation:

$$\int C_{HO\bullet}\,d\,t = \frac{2\,k_{OH_2^-}\,10^{pH-pK_a}}{\sum k_t\,C_S}\sum\int C_{O_3}\,C_{H_2O_2}\,dt = k_{it}\sum\Gamma_i = k_{it}\,\Gamma \tag{11}$$

where k_{it} represents the influence of initiation and termination reactions on the concentration of hydroxyl radicals and Γ, expressed in $mM^{-2}\,s^{-1}$, accounts for the integral in the second member of Eq. 11. The values of Γ were evaluated using the full profile of ozone with data taken every 5 s. If the aggregate TOC is used instead of the concentration of a given individual compound, the combination of Eqs. 9-11 yields the following expression for the logarithmic decay of dissolved carbon:

$$-\ln\frac{TOC}{TOC_o} = k_{TOC}\int C_{HO\bullet}\,d\,t = k_{TOC}\,k_{it}\,\Gamma = k\,\Gamma \tag{12}$$

The use of TOC instead of a given organic compound also justifies ignoring direct ozone reactions in Eq. 3 as they would not reasonably contribute to mineralization.

Fig. 4 shows the result of the least square fitting of the experimental results of three representative experiments to Eq. 12. In all cases, a good fit was obtained on

considering two consecutive periods in the TOC decay pattern. The first one represented rapid mineralization, with the exception of some samples characterized by a low COD/BOD ratio that exhibited an induction period during which TOC remained unchanged. The sample indicated by triangles corresponds to April, which is also represented in Fig. 2a. It shows a period of about 200 s in which TOC was essentially constant. The other experiments shown in Fig. 4 correspond to June (during a rainy week) and July and are representative of samples taken in wet and dry periods respectively.

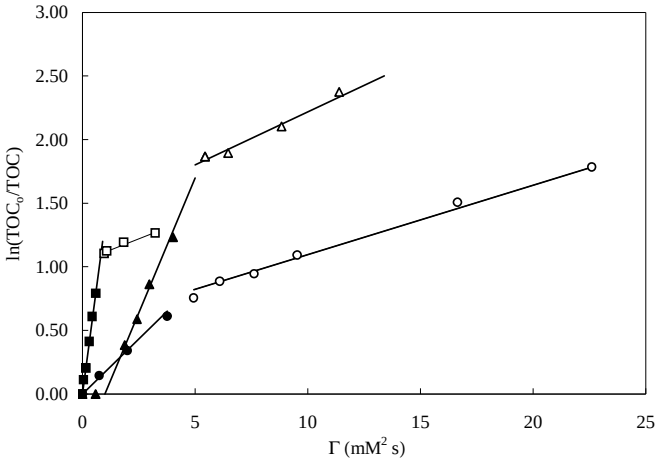

Figure 4. Logarithmic decay of TOC for representative runs corresponding to April (triangles), June (circles) and July (squares) as a function of Γ defined in Eq. (9). Filled and empty symbols indicate the two TOC decay periods at which data were fitted.

The experimental values of the kinetic constant of Eq. 12 are shown in Fig 5a and b for the first (k_1) and second (k_2) fitting periods respectively. In runs showing an initial induction period, this was not considered when computing the kinetic constants of the model. Constants for both periods exhibited important seasonal variation but with larger deviations from the average in the case of k_1. Larger positive deviations corresponded to the dry period in runs with a low amount of dissolved ozone (Fig. 2b) and in which mineralization took place under relatively low ozone exposure and, therefore, small Γ values (see Fig. 4). From the analytical parameters listed in the analysis section, the most significant correlation with the first mineralization constant corresponded to the COD/BOD ratio. The cross-correlation between the time series showed in Fig. 5a was high, allowing COD/BOD to account for more than forty percent of the total variability of k_1, with a minor contribution on the part of chloride content. These facts point to a mineralization kinetics dominated by the nature of the organic matter in wastewater, whose biodegradability also determines the behaviour of dissolved organic carbon towards mineralization in ozonation runs. COD in the SPT effluent was in all cases < 90 mg/L with low variability whereas BOD changed considerably among samples roughly in the 2-20 mg/L range. COD/BOD in the effluent lie between common margins but with some values near or slightly over 20. The non-biodegradable fraction of COD under conventional biological treatments is usually considered the residual COD in the effluent of a properly running wastewater treatment plant. A typical level of non-degradable COD is in the range 40-70 mg/L, of which around 10-20 mg/L is considered residual and non-treatable COD. In the experiments reported in this work, an average COD removal of 65% was attained, with an average COD at the end of ozonation treatments of 28 mg/L. According to these figures, about half of the non-degradable COD can be mineralized by the O_3/H_2O_2 treatment. The removal of BOD was similar, with an average value of 55% and < 2.0 mg/L of residual BOD. The rest can be accounted for by other inorganic substances in solution or by an effect associated with the different behaviour of solids in suspension [35].

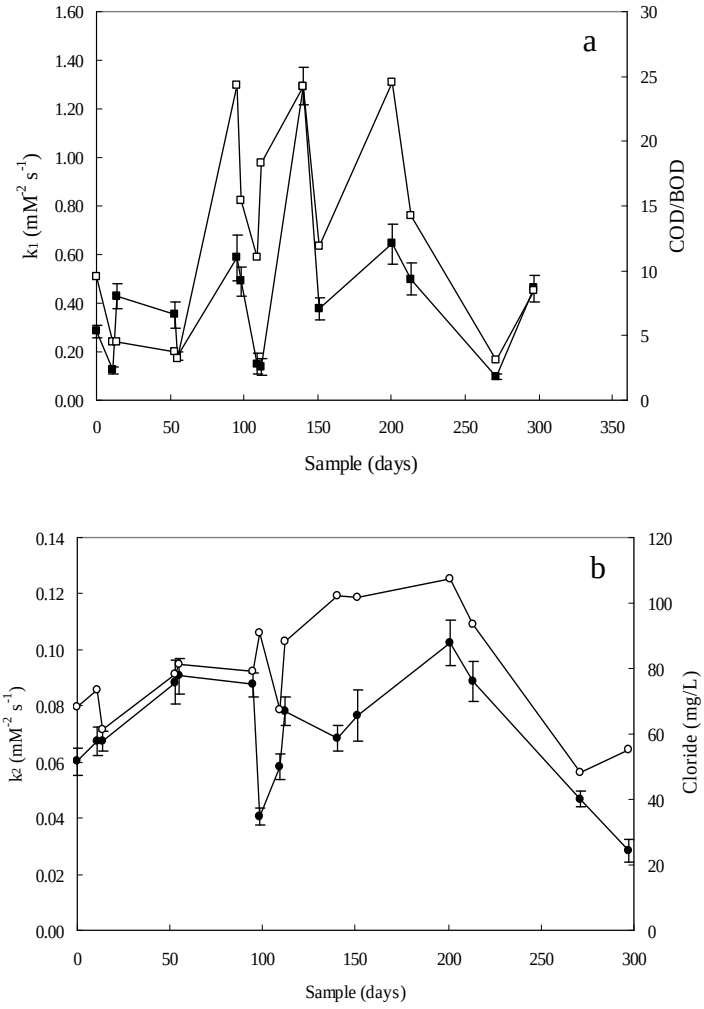

Figure 5. Dependence of reaction kinetic parameters for TOC decay during the first (a) and second (b) fitting period. Filled symbols correspond to k_1 and k_2. Also shown COD/BOD (□) and chloride (○) in wastewater samples.

The second kinetic period showed quite different behaviour and its kinetic constant did not correlate significantly correlated with that of the first. The profile of the time series representing k_2 is shown in Fig. 5b together with that corresponding to the chloride content of wastewater samples. The cross-correlation between the series shown in Fig. 5b was high, so that chlorine content

might explain more than thirty percent of the total variability of k_2. For both constants, the remaining variance is associated with water hardness and, to a lesser extent, to pH. In the case of k_2, sulphate content also had a minor but significant positive influence, whereas higher conductivity and hardness are associated with lower values of k_2. The positive correlation between k_2 and the time series of sulphate and chloride content might be explained by the formation of weak oxidants such as chlorine or sulphate radicals from hydroxyl radicals. These secondary oxidants could extend the effect of the oxidant mixture after the depletion of hydrogen peroxide. To elucidate this point, more research is required, research which falls outside the scope of this paper. Alkalinity did not demonstrate any significant influence on either mineralization constants. The influence of alkalinity of hydroxyl-mediated reactions is well-known, but in this particular case may have been masked by its low variability among samples as indicated in Table 1.

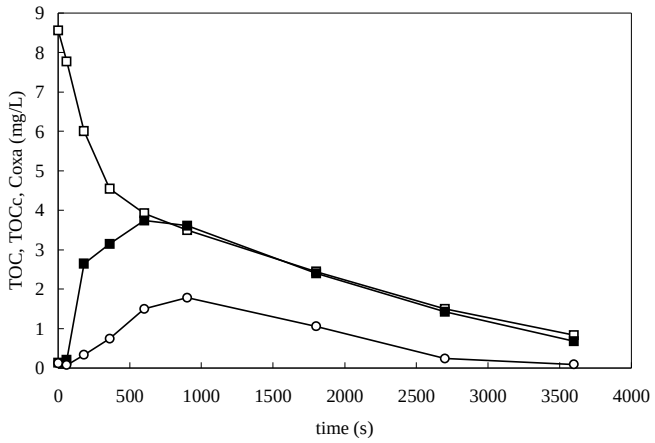

Figure 6. Evolution of experimental TOC (□) and TOC calculated from the concentration of acids formic, acetic and oxalic (■). Empty circles represent the concentration of oxalic acid. In this run, the transition from first to second kinetic period took place at 360 s.

Fig. 6 compares the experimental values of TOC during the ozonation treatment with the dissolved carbon associated with the lower molecular weight carboxylic acids that were analyzed by ionic chromatography, that is, formic, acetic and oxalic acids. Oxalic acid was by far the most predominant except at the early stages of reaction, and exhibited a typical pattern showing a maximum as indicated in Fig. 6. The sample was taken in February with CODo = 62 mg/L and BODo = 6.5 mg/L. The transition from the first rapid mineralization period to the second kinetic stage took place at 360 s, a moment at which most organic carbon measured as TOC took the form of carboxylates. Low molecular weight carboxylic compounds accounted for the totality of the amount of TOC that remained in solution at the end of almost all runs. This result is consistent with the well-known resistance of these compounds to oxidation by ozone [35]. In fact, it has been established that the final oxidation products of many organic compounds are carboxylic acids, a class of compounds that have low reactivity both towards ozone and free radicals [37]. After ozonation, BOD reached values typically below 1 mg/L, whereas COD decreased from 30-80% with samples yielding values as high as 50 m/L. Most COD, about 20 mg/L on average, corresponded to other inorganic compounds such as nitrites or sulphites, while the concentration of chloride was too low to interfere [38]. Other sources of variability can be attributed to solids in suspension and to the formation of oxalic acid, a compound that was reported to inhibit microorganisms that biodegrade organic compounds [39].

Cost analysis and efficiency of mineralization

The model described by Eqs. 10-12 permits the calculation of TOC(t) from continuous measures of $C_{O_3}(t)$ given a dosing strategy for hydrogen peroxide. The amount of ozone being transferred from the gas phase can be calculated from the concentration of dissolved ozone, provided that the concentration in the gas phase is known or accessible to computation. A mass balance to ozone in the gas phase yields:

$$\frac{G}{\varepsilon S}\frac{d\,C_{O_3,g}}{d\,z} = k_L a\left(C^*_{O_3} - C_{O_3}\right) \qquad (13)$$

where ε represents the gas hold-up and z the height from the gas diffuser. Assuming that the concentration of ozone in the liquid phase remains constant during the time a gas bubble needs to rise to the top of the reactor, the integration of Eq. 13 yields:

$$C_{O_3,g}(z) = \left(C^o_{O_3,g} - H\,C_{O_3}\right)e^{-\frac{k_L a\,H\,\varepsilon S}{G\,z}} + H\,C_{O_3} \qquad (14)$$

The correlation of Rischbieter et al. [31] was used to calculate the adimensional Henry's constant: H = 3.97 at 25ºC. The values of $C_{O_3,g}$ for bubbles leaving the reactor were found to differ less than 1% from their initial concentration at the diffuser, $C^o_{O_3,g}$. With constant gas concentration, the instantaneous rate of ozone mass transfer dN_{O_3} can be calculated at any time from the concentration of dissolved ozone as follows:

$$\frac{d\,N_{O_3}}{d\,t} = V\,k_L a\left(C^*_{O_3} - C_{O_3}\right) \qquad (15)$$

The efficiency of the ozonation system to remove dissolved organic carbon can be determined a priori from the model given by Eqs. 10-12 using only information about the concentration of dissolved ozone and the amount of hydrogen peroxide being injected. The instantaneous rate of TOC removal is given by:

$$-\frac{d\,TOC}{d\,t} = k_{TOC}\,TOC\,C_{HO^\bullet} = k\,TOC\,\frac{d\,\Gamma}{d\,t} \qquad (15)$$

A precise evaluation of Γ function is possible due to the accurate measuring of ozone concentration performed with a sampling period of 5 s throughout the run. Combining Eqs. 14 and 15, the number of moles of TOC

removed per mole of ozone being transferred from the gas phase can be calculated as follows:

$$-\frac{d\,N_{TOC}}{d\,N_{O_3}} = \frac{k\,TOC_o\,e^{-k\Gamma}\,\dfrac{d\,\Gamma}{d\,t}}{k_L a\left(C^*_{O_3} - C_{O_3}\right)} \qquad (16)$$

The theoretical number of moles of TOC removed per mole of ozone consumed is shown in Fig. 7 for the same runs represented in Fig. 2. The symbols correspond to experimental TOC values. The good agreement between experimental and theoretical ozone efficiency is noteworthy, especially considering that the theoretical profile can be calculated from a relatively straightforward measure such as dissolved ozone concentration. The dose of hydrogen peroxide is an independent variable that can be handled at will by plant operators, the model only requiring the rate constant *k* to predict the mineralization at a given time. The results show a sharp maximum in mineralization efficiency that always lay in the 150-450 s interval. The dose of ozone transferred during the ozonation, can be calculated from Eq. 14 and represents, for the runs in Fig. 7 and evaluated at the maximum of dN_{TOC}/dN_{O3}, 29.2 mg/L (April) and 23.4 mg/L (Sept.) with a TOC removal of 31% and 17% respectively, representing 10 and 16 mg O_3/mg TOC respectively. For the whole set of runs, the amount of ozone consumed lay in the 9.2-17.7 mg O_3/mg TOC interval, the higher figures corresponding to samples collected during summer whose concentration of dissolved ozone was lower, as shown in Fig. 2.

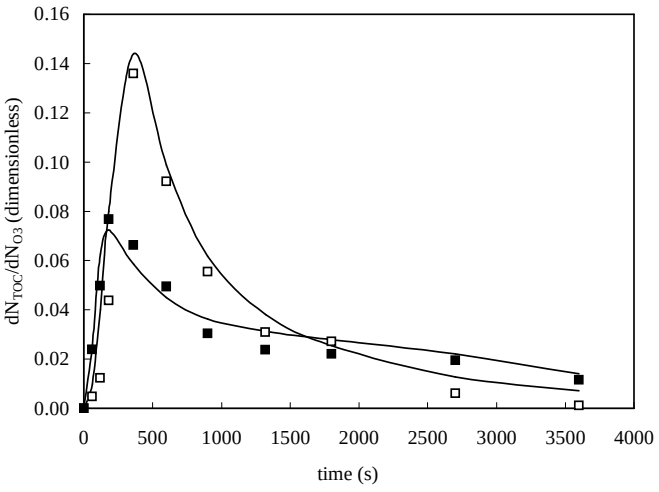

Figure 7. Evolution of the moles of carbon mineralized by unit mole of ozone in runs with wastewater samples taken in April and June. The symbols correspond to experimental values with derivatives obtained by a numerical non-model based procedure.

Data on ozone dosing for O_3/H_2O_2 treatment of wastewater are scarce and difficult to interpret, but there is a certain background on the use of this technique for surface and drinking water. Volk, et al. [40] ozonated surface water with about 15 mg/L of dissolved organic carbon (DOC) that mainly consisted of humic substances and found that for a 10 min treatment with O_3/H_2O_2 the mineralization efficiency was 12.5 mg O_3/mg DOC. Ozone dosing for the ozonation of surface water in processes where mineralization is not pursued, usually lie in the 1–2 mgO_3/mg TOC with a limited degree of mineralization [41]. Muroyama et al. reported an upper limit of 5 min of ozonation for the treatment of drinking water in a bubble column with ozone doses around 3 mg/L [42]. In our work, the amount of ozone transferred was much higher, but also the mineralization was much deeper and mineralization efficiency show similar figures.

The maximum at 2.5-7.5 min corresponded to a period in which a complete removal of a number of micropollutants took place. In a previous paper [26], we reported liquid chromatography-hybrid triple-quadrupole linear ion trap system (LC-QqLIT-MS) analysis of wastewater from the same STP in search of pharmaceuticals and personal care products (PPCP). In that paper, we detected over thirty compounds and metabolites representing 10 μg/L overall, with individual concentrations in the 3–2100 ng/L range. Their fate was followed during ozonation runs with the result that, even under conditions of mild mineralization, the removal efficiencies for most compounds were over >99% after 5 min.

Conclusions

The ozonation treatment of the effluent from the secondary clarifier of an urban STP was carried out by the simultaneous use of ozone and hydrogen peroxide. Kinetic constants for the second order hydroxyl-mediated mineralization process were determined for wastewaters collected throughout a sampling period lasting almost one year. The results showed a TOC decay ranging from 75-100% during one-hour of treatment. In the same conditions but without injecting hydrogen peroxide, the extent of mineralization was always below 35%. In all cases, after a period of 5-15 min, the rate of mineralization changed sharply from a stage of quick mineralization to a second and slower period associated with the reaction of the more refractory compounds. The simple carboxylic acids formic, acetic and oxalic, were identified as the main components of the reaction mixture during the slow reaction period. The rate constant of this period was up to twenty times lower than that of the first part of the ozonation. The rate constants of both periods underwent significant seasonal variability associated to important changes in the amount of dissolved ozone whose concentration was considerably lower during summer. This low amount was probably related to the higher content of nitrate, sulphate and chloride of wastewater during the dry period. The cross-correlation between time series allowed the COD/BOD ratio and the chloride anion content to be identified as the parameters which most contribute to explain the variability of the kinetic constants for the first and second mineralization periods respectively. Also, certain samples characterized by a low COD/BOD ratio had an induction period of a few minutes in which no mineralization

occurred, before then following the same pattern exhibited by other samples. This effect could be attributed to the variable period or time required for the oxidation of complex organic compounds to the final oxidation products. The mineralization model proposed in this work can be used to estimate the ozone dosing required to achieve a certain amount of TOC removal by using exclusively the information from the concentration profile of dissolved ozone. The efficiency of the use of ozone increased during a 150-450 s period at the beginning of the runs to steadily decay thereafter. At maximum efficiency, the amount of ozone consumed per unit mass of TOC removed lay in the 9.2-17.7 mg O_3/mg TOC interval, representing a mineralization rate in the 17-31% range. These short treatments proved to yield high removal efficiencies of +99% for most pharmaceuticals found in wastewater with concentrations in the order of ppb or ppt. During a one-hour treatment complete mineralization required, whenever possible, ozone doses of up to 150 mg/L. These figures are certainly higher that those usually encountered in O_3/H_2O_2 treatments of drinking water, but similar to the limited data available on wastewater treatment.

Nomenclature

C_{O_3} concentration of dissolved ozone (M)
$C^*_{O_3}$ equilibrium concentration of dissolved ozone (M)
$C_{O_3 g}$ concentration of ozone in gas phase (M)
$C^o_{O_3 g}$ concentration of ozone in the gas leaving the diffuser (M)
$C_{H_2O_2}$ concentration of hydrogen peroxide (M)
$C_{HO^\bullet}$ concentration of hydroxyl radicals (M)
C_{HO^-} concentration of hydroxide anion (M)
$C_{HO_2^-}$ concentration of hydroperoxide anion (M)
C_P concentration of a given compound (M)
C_S concentration of radical scavengers (M)
D_{O_3} diffusivity of ozone in water ($m^2\ s^{-1}$)
G gas flow rate ($m^3\ s^{-1}$)
H Henry's law constant (dimensionless)
$k_{HO_2^-}$ kinetic constant of the reaction between ozone and hydroperoxide anion ($M^{-1}\ s^{-1}$)
k_{HO^-} kinetic constant of the reaction between ozone and hydroxide anion ($M^{-1}\ s^{-1}$)
k_L Liquid phase individual mass transfer coefficient ($m\ s^{-1}$)
k_La volumetric mass transfer coefficient (s^{-1})
k_P kinetic constant for the indirect ozonation of a given compound ($M^{-1}\ s^{-1}$)
k_{TOC} mineralization kinetic constant ($M^{-1}\ s^{-1}$)
k_t kinetic constant of termination reactions ($M^{-1}\ s^{-1}$)
k_{it} constant defined in Eq. 9 (M^{-1})
k kinetic constant defined in Eq. 10 ($M^{-2}\ s^{-1}$)
k_1 kinetic constant for the first mineralization period ($M^{-2}\ s^{-1}$)
k_2 kinetic constant for the second mineralization period ($M^{-2}\ s^{-1}$)
N number of pulses of hydrogen peroxide
N_{O_3} moles of ozone (mol)
S section of the reactor (m^2)
V volume occupied by the liquid phase (m^3)
z height from the diffuser (m)

Greek letters
Γ function defined in Eq. 9 (M^2 s)
ε gas-hold up (dimensionless)

Acknowledgements

The authors express their gratitude to the Ministry of Education of Spain (Contracts CTM2005-03080/TECNO and CSD2006-00044) and to the DGUI de la Comunidad de Madrid (Contract 0505/AMB-0395).

References

[1] EC, Directive of the European Parliament and of the Council 2000/60/EC establishing a framework for community action in the field of water policy, Official Journal, 2000, C513, 23/10/2000.
[2] Environmental Protection Agency, US EPA, Guidelines for Water Reuse, EPA/625/R-04/108 U.S., Agency for International Development ashington, DC, 2004.
[3] J.H.J.M. van der Graaf, J. de Koning, A.M. Ravazzini, V. Miska, Treatment matrix for reuse of upgraded wastewater, Water Sci. Technol.: Water Supply, 5 (2005) 87–94.
[4] T.A. Ternes, Occurrence of drugs in German sewage treatment plants and rivers, Water Res., 32 (1998) 3245–60.
[5] M. Carballa, F. Omil, J.M. Lema, M. Llompart, C. García-Jares, I. Rodríguez, M. Gómez, T. Ternes, Behavior of pharmaceuticals, cosmetics and hormones in a sewage treatment plant, Water Res., 38 (2004) 2918-2926.
[6] F. Gagné, C. Blaise, C. André, Occurrence of pharmaceutical products in a municipal effluent and toxicity to rainbow trout (Oncorhynchus mykiss) hepatocytes, Ecotoxicol. Environ. Saf., 64 (2006) 329-336.
[7] P.H. Roberts, K.V. Thomas, The occurrence of selected pharmaceuticals in wastewaters effluent and surface waters of lower Tyne catchment, Sci. Total Environ., 356 (2006) 143–153.
[8] J.H. Al-Rifai, C.L. Gabelish, A.I. Schäfer, Occurrence of pharmaceutically active and non-steroidal estrogenic compounds in three different wastewater recycling schemes in Australia, Chemosphere, 69 (2007) 803-815.
[9] H. Kusic, N. Koprivanac, A.L. Bozic, Minimization of organic pollutant content in aqueous solution by means of AOPs: UV- and

ozone-based technologies, Chem. Eng. J., 123 (2006) 127-137.
[10] N.C. Shang, Y.H. Yu, H.W. Ma, C.H. Chang, M.L. Liou, Toxicity measurements in aqueous solution during ozonation of mono-chlorophenols, J. Environ. Manage., 78 (2006) 216–222.
[11] R.F. Dantas, M. Canterino, R. Marotta, C. Sans, S. Esplugas, R. Andreozzi, Bezafibrate removal by means of ozonation: Primary intermediates, kinetics, and toxicity assessment, Water Res., 41 (2007) 2525-2532.
[12] T.A. Larsen, J. Lienert, A. Joss, H. Siegrist, How to avoid pharmaceuticals in the aquatic environment, J. Biotechnol., 113 (2004) 295-304.
[13] S. Esplugas, J. Giménez, S. Contreras, E. Pascual, M. Rodríguez, Comparison of different advanced oxidation processes for phenol degradation, Water Res., 36 (2002) 1034-1042.
[14] K. Ikehata, N.J. Naghashkar, M.G. El-Din, Degradation of aqueous pharmaceuticals by ozonation and advanced ozonation processes: A review, Ozone: Sci. Eng., 28 (2006) 353-414.
[15] P.R. Gogate, A.B. Pandit, A review of imperative technologies for wastewater treatment I: oxidation technologies at ambient conditions, Adv. Environ. Res., 8 (2004) 501-551.
[16] P.R. Gogate, A.B. Pandit, A review of imperative technologies for wastewater treatment II: Hybrid methods, Adv. Environ. Res., 8 (2004) 553-597.
[17] S. Staehelin, J. Hoigné, Reaktionsmechanismus und Kinetik des Ozonzerfalls in Wasser in Gegenwart organischer Stoffe, Vom Wasser, 61 (1983) 337-348.
[18] H. Tomiyasu, H. Fukutomi, G. Gordon, Kinetics and mechanism of ozone decomposition in basic aqueous solution, Inorg. Chem., 24 (1985) 2962-2966.
[19] J. Hoigné, Chemistry of aqueous ozone and transformation of pollutants by ozone and advanced oxidation processes, in: J. Hrubec (Ed.), The Handbook of Environmental Chemistry, vol. 5, part C, Quality and Treatment of Drinking Water, Part II, Springer, Berlin Heidelberg, 1998.
[20] C. Yang, Y.R. Xu, K.C. Teo, N.K. Goh, L.S. Chia, R.J. Xie, Destruction of organic pollutants in reusable wastewater using advanced oxidation technology, Chemosphere, 59 (2005) 441-445.
[21] M.L. Gómez, M.J. Martínez, S. Lacorte, A.R. Fernández-Alba, A. Agüera, Pilot survey monitoring pharmaceuticals and related compounds in a sewage treatment plant located on the Mediterranean coast, Chemosphere, 66 (2007) 993-1002.
[22] I.. Muñoz, A. Rodríguez, R. Rosal, A.R. Fernández-Alba, Life Cycle Assessment of urban wastewater reuse with ozonation as tertiary treatment. A focus on toxicity-related impacts, Sci. Total. Environ., in press.
[23] P. Ormad, L.S. Cortés, A. Puig, J.L. Ovelleiro, Degradation of organochlorine compounds by O_3 and O_3/H_2O_2, Water Res., 31 (1997) 2387-2391.
[24] S. Liang, R.S. Yates, D.V. Davis, S.J. Pastor, S.L. Palencia, J.M. Bruno, Treatability of MTBE-contaminated groundwater by ozone and peroxone, J. Am. Water Works Assoc., 93 (2001) 110-120.
[25] F.J. Beltrán, 2004. Ozone reaction kinetics for water and wastewater systems. CRC Press, Boca Raton, pp 178-179.
[26] R. Rosal, A. Rodríguez, J.A. Perdigón-Melón, M. Mezcua, A. Agüera, M.D. Hernando, P. Letón, E. García-Calvo, A.R. Fernández-Alba, Removal of pharmaceuticals and kinetics of mineralization by O_3/H_2O_2 in a biotreated municipal wastewater, Water Res., 42 (2008) 3719-3728.
[27] R. Rosal, A. Rodríguez, M.S. Gonzalo, E. García-Calvo, Catalytic ozonation of naproxen and carbamazepine on titanium dioxide, Appl. Catal., B, 84, 48–57 (2008).
[28] M.S. Chandrakanth, G.L. Amy, Effects of NOM source variations and calcium complexation capacity on ozone-induced particle destabilization, Water Res., 32 (1998) 115–124.
[29] K.L. Rakness, L.D., Demers, B.D. Blank, D.J., Henry, Gas phase ozone concentration comparisons from a commercial UV meter and KI wet-chemistry tests, Ozone: sci. Eng., 18 (1996) 231-249.
[30] G.M. Eisenberg, Colorimetric determination of hydrogen peroxide, Ind. Eng. Chem., 15 (1948) 327-328.
[31] E. Rischbieter, H. Stein, A. Shumpe, Ozone Solubilities in Water and Aqueous Salt, J. Chem. Eng. Data, 45 (2000) 338-340.
[32] H. Paillard, R. Brunet, M. Dore, Optimal conditions for applying an ozone-hydrogen peroxide oxidising system, Water Res., 22 (1988) 91-103.
[33] F.J. Beltrán, J.F. García, P.M. Álvarez, J. Rivas, Aqueous degradation of atrazine and some of its main by-products with ozone hydrogen peroxide, J. Chem. Technol. Biotechnol., 71 (1998) 345-355.
[34] P.H. Calderbank, M.B. Moo-Young, The continuous phase heat and mass transfer properties of dispersions, Chem. Eng. Sci., 16 (1961) 39-54.
[35] J. Lu, X. Wang, B. Shan, X. Li, W. Wang, Analysis of chemical compositions contributable to chemical oxygen demand (COD) of oilfield produced water, Chemosphere, 62 (2006) 322–331.
[36] S. Contreras, M. Rodríguez, F. Momani, C. Sans, S. Esplugas, Contribution of the ozonation pre-treatment to the biodegradation of aqueous solutions of 2,4-dichlorophenol, Water Res., 37 (2003) 3164–3171.
[37] G.V. Buxton, C.L. Greenstock, W.P. Hwlman, A.B. Ross, Critical review of rate constants for reactions of hydrated electrons, hydrogen atoms and hydroxyl radicals (OH/O^-) in aqueous solution, J. Phys. Chem. Ref. Data, 17 (1988) 513-886.

[38] L. Zhu, Y. Chen, Y. Wu, X. Li, H. Tang, A surface-fluorinated-TiO_2–$KMnO_4$ photocatalytic system for determination of chemical oxygen demand, Anal. Chim. Acta, 571 (2006) 242-247.
[39] M.M. Ballesteros, J.A. Sánchez, F.G. Acién, J.L. García, J.L. Casas, S. Malato, A kinetic study on the biodegradation of synthetic wastewater simulating effluent from an advanced oxidation process using *Pseudomonas putida* CECT 324, J. Hazard. Mater., 151 (2008) 780–788.
[40] C. Volk, P. Roche, J.C. Joret, H. Paillard, Comparison of the effect of ozone, ozone-hydrogen peroxide system and catalytic ozone on the biodegradable organic matter of a fulvic acid solution, Water Res., 3 (1997) 650-656.
[41] B. Seredynska-Sobecka, A. Tomaszewska, A.W. Morawski, Removal of micropollutants from water by ozonation/biofiltration process, Desalination, 182 (2005) 151–157.
[42] K. Muroyama, M. Yamasaki, M. Shimizua, E. Shibutania, T. Tsuji, Modeling and scale-up simulation of U-tube ozone oxidation reactor for treating drinking water, Chem. Eng. Sci., 60 (2005) 6360–6370.